ChemComm

RSC Publishing

COMMUNICATION

View Article Online
View Journal | View Issue

Cite this: *Chem. Commun.*, 2013, **49**, 9443

Received 24th June 2013,
Accepted 15th August 2013

DOI: 10.1039/c3cc44742a

www.rsc.org/chemcomm

Nano-size effects on CuO/TiO_2 catalysts for highly efficient H_2 production under solar light irradiation†

Dharani Praveen Kumar,[a] Muthukonda V. Shankar,*[a] Murikinati Mamatha Kumari,[a] Gullapelli Sadanandam,[b] Basavaraju Srinivas[b] and Valluri Durgakumari*[b]

Solar light induced interfacial charge transfer of electrons from TiO_2 to CuO in a water–glycerol mixture produced 99 823 μmol h^{-1} $g^{-1}_{catalyst}$ of hydrogen gas. The dispersed CuO/TiO_2 photocatalyst in solution exhibited uni-directional electron flow and capture at the Schottky barrier facilitating charge separation and electron transfer resulting in enhanced H_2 production performance.

Hydrogen (H_2) generation from solar photocatalytic water splitting is a clean process, performed under ambient conditions. Hydrogen reacts with oxygen in fuel cells, produces electricity and serves the societal demand.[1] For commercial H_2 production researchers are working on the development of efficient photocatalysts and reactors with a targeted 10% quantum yield under visible light.[2] Among the important criteria identified for efficient photocatalytic water splitting are: (i) energy band configuration and (ii) surface properties. They greatly influence the band edge potential, visible light absorption, charge carrier separation, surface reactions, chemical stability and corrosion resistance.[2] Significant progress has been made for efficient overall water splitting into H_2 and O_2 using novel active photocatalysts under solar light irradiation.[3] Among the systems reported, TiO_2 has been the most attractive due to its appropriate energy band potential, stability, non-toxicity, low-cost and easy availability. However, poor visible light absorption and fast charge carrier (electron–hole) recombination limit its application potential. It is known that the use of heterojunction based semiconductor composites is an effective route to overcome the above barriers and improve the catalytic efficiency. Copper (Cu^0, Cu^{2+}, CuO, Cu_2O) based TiO_2 heterojunction catalysts showed efficient H_2 generation, superior even to those of several noble-metal loaded TiO_2 systems.[4,5,6b] They possess significant advantages in photoconversion efficiency and promote electron–hole separation *via* an interfacial charge transfer process. Copper oxides have several benefits, such as narrow band-gap, stability, affordability, and they are abundantly available in nature.

Nanostructured photocatalysts exhibited improved performance compared to nanoparticles in the water splitting process.[2a,c] Particularly, the 1-D TiO_2 nanostructure with a tubular structure and hollow inside (porous) is of great potential in photocatalysis.[7a–d] Such catalysts showed a large surface area, extended energy band potential and electrons delocalized along the uni-directional axis. Enhancement in the H_2 production rate with TiO_2 nanostructures modified with dopants,[8a,b] sensitizers,[8c] co-catalysts[8d] and scavengers[8e] was reported. Our group's success in enhancement of photocatalytic H_2 production (Table 1 entries 4–6) using Cu_2O/TiO_2 photocatalyst encouraged us to the present approach on TiO_2 nanotube material. The scope of the present work is execution of the heterojunction concept on nanotube and quantum dot composites. Here we report the synthesis of CuO deposition over TiO_2 nanotubes and optimization of parameters for highly efficient H_2 production. In the bio-diesel production process the glycerol by-product generated is chosen as the scavenger for H_2 production as it provides a sustainable way to utilize the industrial by-product.

TiO_2 nanotubes were synthesized using micrometer sized TiO_2 particles as the precursor with some modifications in the reported procedure.[9a] The wet-impregnation method was adopted for preparation of $CuO–TiO_2$ nanocomposites using copper nitrate solution.[6b] The activity measurements were

Table 1 Comparison of H_2 production rates

Sl No.	Photocatalyst	Scavenger	Light source	H_2 production μmol h^{-1} g^{-1}_{cat}	Ref.
1	$NiO/NaTaO_3$:La	Methanol	Hg	38 400	9*b*
2	Pt/TiO_2	Methanol	Hg	21 350	9*c*
3	CuO/TiO_2NT	Methanol	Hg	71 600	9*d*
4	Ag_2O/TiO_2	Methanol	Solar	3350	6*a*
5	Cu_2O/TiO_2	Glycerol	Solar	20 060	6*b*
6	CoO/TiO_2	Glycerol	Solar	11 021	6*c*
7	CuO/TiO_2NT	Glycerol	Solar	99 823	Present report

[a] *Nano Catalysis Research Lab, Department of Materials Science & Nanotechnology, Yogi Vemana University, Kadapa 516003, India. E-mail: shankarnano@gmail.com; Fax: +91-8562225419; Tel: +91-9966845899*

[b] *Inorganic and Physical Chemistry Division, Indian Institute of Chemical Technology (IICT), Hyderabad 500607, India. E-mail: durgakumari@iict.res.in; Fax: +91-40-27160921; Tel: +91-40-27193165*

† Electronic supplementary information (ESI) available: Experimental, materials characterization, results and Fig. S1–S6. See DOI: 10.1039/c3cc44742a

carried out in a quartz reactor under ambient conditions and solar light irradiation. The photocatalysts used for H_2 generation experiments are given below:

Photocatalysts	
TiO_2 Degussa-P25	TNP
Calcined TiO_2 nanotube	TNT
0.1 wt% Cu-loaded TNT	CuTNT-1
0.5 wt% Cu-loaded TNT	CuTNT-2
1.0 wt% Cu-loaded TNT	CuTNT-3
1.5 wt% Cu-loaded TNT	CuTNT-4
2.0 wt% Cu-loaded TNT	CuTNT-5

The X-ray diffraction patterns (Fig. S1, ESI†) of TNP, TNT and CuTNT-4 materials reveal that the anatase–rutile mixed phase exists in TiO_2 with characteristic diffraction peaks (101) and (110) observed at 2θ = 25.4 and 27.5 respectively. The CuTNT-4 photocatalyst showed intense peaks due to improved crystallinity and no characteristic peak exists for copper species due to fine dispersion of quantum sized particles. The TEM image (Fig. S2a (ESI†)) of TNT showed tubular shapes, hollow in nature and open-ended on both sides. The tube lengths and diameters were 300 to 400 nm and 8–12 nm respectively. The TEM image (Fig. S2b, ESI†) of CuTNT-4 showed clear evidence for CuO quantum dots (<10 nm) deposited on the surface of nanotubes without damaging the tubular structure.

The diffuse reflectance UV-Vis spectrum (Fig. S3, ESI†) of photocatalysts reveals that TNT absorption is slightly blue shifted compared with TNP due to quantum size effects. This has pushed the band edges and increased the effective band gap to 3.2 eV. The CuTNT-4 catalyst appears pale yellow-blue in colour and showed extended absorption towards the visible region, E_g = 3.05 eV due to the CuO content. The observed shift is likely due to nanoheterojunction formed between CuO and TNT interface. Given potential energy level of CuTNT-4, it is clear that CuO acts only as co-catalyst and not acts as inorganic visible light absorption sensitizer.

The specific surface areas of the photocatalysts are 220, 157 and 48 $m^2\ g^{-1}$ for TNT, CuTNT-4 and TNP respectively. The chemical composition of the CuTNT-4 photocatalysts and chemical status of copper was analysed using XPS spectroscopy (Fig. S4, ESI†). The data for CuTNT-4 indicate that Ti, O, Cu and C elements are observed and their respective photoelectron peaks appear at binding energies of 459.4 (Ti2p), 530.6 (O1s), 933.7 (Cu2p) and 284.6 eV (C1s). The atomic ratio of Ti to O is about 1:2, which is in good agreement with the nominal atomic composition of TiO_2. These binding energies indicate that the oxidation state of copper present on the surface of TiO_2 is +2. The copper peak comes from CuO. This is also in agreement with previous reports.[6b]

To begin with, optimization of catalyst loading was studied from 1 to 100 mg with TNT as the photocatalyst. Fig. 1 displays the increase in the volume of H_2 generated with irradiation time and the best results were observed with 5 mg catalyst and the rate of H_2 production was 4625 μmol h^{-1} g^{-1}_{cat}. The present results reveal that approx. 10% of the catalyst amount *i.e.* 0.1 g L^{-1} is

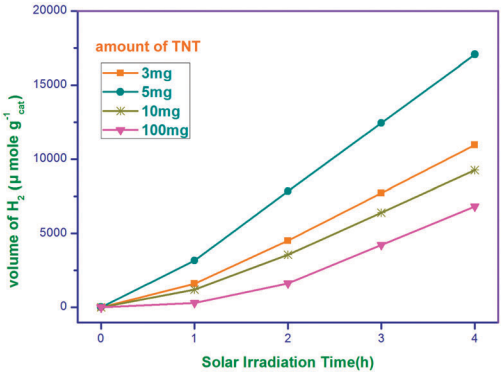

Fig. 1 TNT photocatalyst optimization for efficient H_2 production.

sufficient for efficient H_2 production rates under solar light irradiation. This is the best active photocatalyst system for hydrogen production rate ever obtained using the smallest amount of photocatalyst. Similarly, an earlier report demonstrates that the quantum yield doubled upon decreasing the amount of a highly efficient photocatalyst from 0.5 to 0.05 g (Table 1, entry 1). Thus our results indicate that our catalyst is well-dispersed at the optimal catalyst amount resulting in effective light utilization for oxidation–reduction reactions.

Optimization of copper with TNT catalysts for efficient H_2 generation was performed and results are displayed in Fig. S5 (ESI†). It is observed that increase in copper loading results in higher H_2 production upto 1.5 wt%, beyond which the opposite effect was observed. Above the monolayer dispersion, agglomeration of copper species on the nanotube surface may produce large size CuO nanoparticles having a low band potential, which is inefficient for H_2 production besides the light screening effect. At optimized conditions the H_2 production rate was found to be 99 823 μmol h^{-1} g^{-1}_{cat}.

Fig. 2 displays a comparison of different photocatalysts for H_2 generation under solar irradiation. The efficiency of photocatalytic H_2 generation is in the following order CuTNT-4 > TNT > TNP. In the TNP photocatalyst, the majority of the generated charge carriers undergo fast recombination and only a fraction is utilized for H_2 generation. The observed significant improvement in H_2 evolution is likely due to delocalization of electrons along

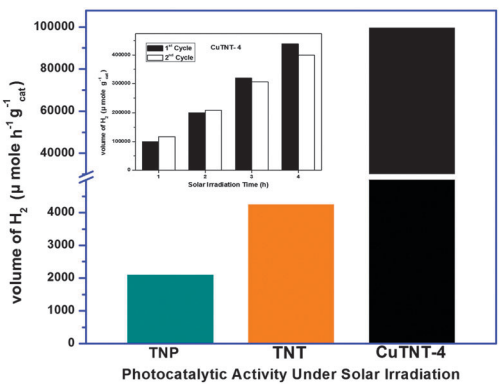

Fig. 2 Evaluation of photocatalytic activity for H_2 generation under solar irradiation. Inset: CuTNT-4 sustainability.

the axis of nanotube.[9b] CuTNT-4 exhibited largest H_2 production as a cumulative effect of photogenerated electrons and efficient transfer of electrons to CuO sites followed by proton reduction. CuTNT-4 has the best photocatalytic hydrogen evolution rate ever obtained for Ti-based catalysts which is about five times larger than the best reported values so far using glycerol as the sacrificial agent. This has favourable band-edges that straddle the redox potential of water photoelectrolysis and also exhibit stability and recyclability in the literature compared with similar materials (Table 1). To evaluate the sustainability of the photocatalysts, tests were also conducted by evacuating the produced gases at regular intervals (4 h); a continuous and stable photocatalytic activity was observed as shown in Fig. 2 inset. The greater activity of CuTNT-4 compared to earlier results on Cu_2O–TiO_2 composites is due to nanosized effects.

The highly efficient photocatalytic activity of CuTNT-4 is ascribed to the following reasons: (A) efficient solar light absorption through (i) minimized light reflection by photocatalyst and (ii) absorbed photons having high efficiency for generation of excited charge carriers instead of heat. (B) Fast charge carrier transfer and water splitting reactions due to (iii) n-type electrical conductivity of CuTNT-4 being increased due to the 1-D structure (iv) efficient separation and fast reduction of protons to H_2 by quantum size CuO and (v) effective adsorption of reactants involved for charge carrier utilization and desorption of products.

The possible mechanism for highly efficient H_2 production under solar irradiation using CuTNT-4 photocatalysts is as follows (Fig. S6, ESI†): the band potentials of CuO and TNT are sufficient for proton reduction for H_2 generation. The photogenerated electrons transferred from the CB of TiO_2 nanotubes to CuO nanoparticles, due to the lower potential of the CB energy level. Accumulation of excess of electrons at CuO causes a negative shift in the Fermi level that leads to Cu_2O formation. This facilitated interfacial electron transfers from Cu_2O to solution resulting in H_2 production. Meanwhile holes accumulated in the VB of CuO/Cu_2O and TiO_2 could be consumed by the sacrificial agent glycerol or by generating the hydroxyl radical ($^{\bullet}OH$) reaction with H_2O molecules. Consequently, this process reduced the recombination of photogenerated electron–hole pairs and facilitated enhanced rate of H_2 production.

In summary, we have prepared a novel nano-heterojunction composite photocatalyst, CuTNT using micrometer sized TiO_2 bulk particles. It is claimed that a highly efficient H_2 production rate is recorded under natural solar irradiation using 0.1 g L^{-1} of the CuTNT-4 photocatalyst. It exhibited stability and efficiency for repeated use. The highly efficient photocatalyst CuTNT-4 has produced 399 292 μmol $g^{-1}{}_{cat}$ within 4 h. Both the nanotubular morphology of TiO_2 and the quantum size of CuO are responsible for high efficiency under solar light irradiation. Here CuO acts as an efficient co-catalyst for enhanced H_2 production. To date, the hydrogen production efficiency of CuTNT-4 is the largest using glycerol as the sacrificial agent. Further work is in progress for mechanistic studies and to scale-up the reactors for large scale solar photocatalytic water splitting.

Financial support from Ministry of New and Renewable Energy (MNRE), New Delhi, India (No. 103/163/2009/NT), is gratefully acknowledged. Dr Shankar is indebted to Dr M. Subrahmanyam, Emeritus Scientist of IICT, for providing valuable insights during scientific discussion. Further, he acknowledges the unstinted support extended by Prof. A. Ramachandra Reddy, former vice-chancellor, Prof. K. Krishna Reddy, Dean of Physical Sciences, and Prof. M. Ramakrishna Reddy, Registrar of Yogi Vemana University, for this research work.

Notes and references

1 (*a*) J. S. Lee, *Catal. Surv. Asia*, 2005, **9**, 217–228; (*b*) P. Tseng, J. Lee and P. Eriley, *Energy*, 2005, **30**, 2703–2720; (*c*) E. Serrano a, G. Rus and J. G. Martínez, *Renew. Sustainable Energy Rev.*, 2009, **13**, 2373–2384.

2 (*a*) A. Kudo and Y. Miseki, *Chem. Soc. Rev.*, 2009, **38**, 253–278; (*b*) X. Chen, S. Shen, L. Guo and S. S. Mao, *Chem. Rev.*, 2010, **110**, 6503–6570; (*c*) H. Tong, S. Ouyang, Y. Bi, N. Umezawa, M. Oshikiri and J. Ye, *Adv. Mater.*, 2012, **24**, 229–251; (*d*) Y. Quab and X. F. Duan, *Chem. Soc. Rev.*, 2013, **42**, 2568–2580; (*e*) C. Huang, W. Yao, A. T. Raissi and N. Muradov, *Sol. Energy*, 2011, **85**, 19–27.

3 (*a*) Z. Zou, J. Ye and K. Sayama, *Nature*, 2001, **414**, 625–627; (*b*) R. Abe, T. Takata, H. Sugihara and K. Domen, *Chem. Commun.*, 2005, 3829–3831; (*c*) K. Maeda, K. Teramura and K. Domen, *J. Catal.*, 2008, **254**, 198–204; (*d*) S. S. Khine Ma, K. Maeda and K. Domen, *Catal. Sci. Technol.*, 2012, **2**, 818–823; (*e*) N. Baliarsingh, L. Mohapatra and K. Parida, *J. Mater. Chem. A*, 2013, **1**, 4236–4243; (*f*) U. Diebold, *Nat. Chem.*, 2011, **3**, 271–272.

4 (*a*) X. Qiu, M. Miyauchi, H. Yu, H. Irie and K. Hashimoto, *J. Am. Chem. Soc.*, 2010, **132**, 15259–15267; (*b*) H. Yu, H. Irie and K. Hashimoto, *J. Am. Chem. Soc.*, 2010, **132**, 6898–6899; (*c*) S. Xu and D. D. Sun, *Int. J. Hydrogen Energy*, 2009, **34**, 6096–6104; (*d*) L. S. Yoong, F. K. Chong and B. K. Dutta, *Energy*, 2009, **34**, 1652–1661; (*e*) S. Xu, J. Ng, X. Zhang, H. Bai and D. D. Sun, *Int. J. Hydrogen Energy*, 2010, **35**, 5254–5261; (*f*) W. J. Foo, C. Zhangbc and G. W. Ho, *Nanoscale*, 2013, **5**, 759–764; (*g*) X. Fan, Q. Zhang and Y. Wang, *Phys. Chem. Chem. Phys.*, 2013, **15**, 2632–2649.

5 (*a*) S. Xu, J. Ng, A. J. Du, J. Liu and D. D. Sun, *Int. J. Hydrogen Energy*, 2011, **36**, 6538–6545; (*b*) S. Xu, A. J. Du, J. Liu, J. Ng and D. D. Sun, *Int. J. Hydrogen Energy*, 2011, **36**, 6560–6568; (*c*) H. Dang, X. Dong, Y. Dong, Y. Zhang and S. Hampshire, *Int. J. Hydrogen Energy*, 2013, **3**(8), 2126–2135; (*d*) S. S. Lee, H. Bai, Z. Liu and D. D. Sun, *Water Res.*, 2013, **47**, 4059–4073.

6 (*a*) K. Lalitha, J. Krishna Reddy, M. V. P. Sharma, V. Durga Kumari and M. Subrahmanyam, *Int. J. Hydrogen Energy*, 2010, **35**, 3991–4001; (*b*) K. Lalitha, G. Sadanandam, V. Durga Kumari, M. Subrahmanyam, B. Sreedhar and N. Y. Hebalkar, *J. Phys. Chem. C*, 2010, **114**, 22181–22189; (*c*) G. Sadanandam, K. Lalitha, V. Durga Kumari, M. V. Shankar and M. Subrahmanyam, *Int. J. Hydrogen Energy*, 2013, **38**, 9655–9664.

7 (*a*) O. Rosseler, M. V. Shankar, M. Du, L. Schmidlin, N. Keller and V. Keller, *J. Catal.*, 2010, **269**, 179–190; (*b*) M. A. Khan, M. S. Akhtar, S. I. Woo and O. B. Yang, *Catal. Commun.*, 2008, **10**, 1–5; (*c*) Q. Chen, W. Z. Zhou, G. H. Du and L. M. Peng, *Adv. Mater.*, 2002, **14**, 1208–1211; (*d*) D. V. Bavykin, V. N. Parmon, A. A. Lapkin and F. C. Walsh, *J. Mater. Chem.*, 2004, **14**, 3370–3377.

8 (*a*) M. V. Shankar and J. Ye, *Catal. Commun.*, 2009, **11**, 261–265; (*b*) J. Krishna Reddy, G. Suresh, C. H. Hymavathi, V. Durga Kumari and M. Subrahmanyam, *Catal. Today*, 2009, **141**, 89–93; (*c*) Z. Jin, X. Zhang, Y. Li, S. Li and G. Lu, *Catal. Commun.*, 2007, **8**, 1267–1273; (*d*) L. Zhang, B. Tian, F. Chen and J. Zhang, *Int. J. Hydrogen Energy*, **37**, 17060–17067; (*e*) F. Guzman, S. S. C. Chuang and C. Yang, *Ind. Eng. Chem. Res.*, 2013, **52**, 61–65.

9 (*a*) T. Kasuga, M. Hiramatsu, A. Hoson, T. Sekino and K. Nihara, *Langmuir*, 1998, **14**, 3160–3163; (*b*) H. Kato, K. Asakura and A. Kudo, *J. Am. Chem. Soc.*, 2003, **125**, 3082–3089; (*c*) A. Naldoni, M. D. Arienzo, M. Altomare, M. Marelli, R. Scotti, F. Morazzoni, E. Selli and V. D. Santo, *Appl. Catal., B*, 2013, **130–131**, 239–248; (*d*) S. Xu, A. J. Du, J. Liu, J. Ng and D. D. Sun, *Int. J. Hydrogen Energy*, 2011, **36**, 6560–6568.